Ellipsometric Study of Dissolution of Anodic WO_3 Films in Aqueous Solutions. 2. Reaction Mechanism

M. A. Pérez* and M. López Teijelo

Facultad de Ciencias Químicas, INFIQC-Departamento de Fisicoquímica, Universidad Nacional de Córdoba, Haya de la Torre y Medina Allende, Ciudad Universitaria, 5000 Córdoba, Argentina

Received: March 3, 2005; In Final Form: July 15, 2005

The present work demonstrates that the dissolution of anodic WO_3 can be described in terms of general mechanisms already used to account for the physicochemical processes involved in the dissolution of oxides of other metals. The chemical dissolution of anodic WO_3 films is characterized by in situ ellipsometry, which has proven to be a suitable technique for studying the processes taking place.[1] The capability of ellipsometry for distinguishing between thickness decrease and hydration and generation of porosity/roughness helps to analyze the thickness range within which reliable kinetic information can be obtained. The dissolution rate law found for anodic WO_3 does not depend on the oxide thickness. The dissolution of anodic WO_3 films includes hydration and roughening, besides thickness decrease, and is kinetically controlled by the OH^- concentration at the oxide/electrolyte interface. Apart from OH^-, the specific nature of electrolyte anions seems to play no kinetic role, except in promoting porosity/roughness.

1. Introduction

Tungsten oxide (WO_3) is as an attractive material to be used in manufacturing optical devices, although oxide dissolution and erosion during charge/discharge cycles have limited its use in mass production.[2] Capacitance measurements have been mainly employed for characterizing the chemical dissolution of oxide films in different electrolytic media.[3−6] However, capacitance/time experiments have led to different rate laws depending on the studied electrolyte. The dissolution of anodic WO_3 films in H_2SO_4/Na_2SO_4 and acetic acid/acetate solutions obeys a rate law with a first-order dependence on film thickness,[3,6] whereas in H_3PO_4/NaH_2PO_4 and HCl/NaCl solutions, the rate law does not depend on oxide thickness (zero-order kinetics).[4,5] This would suggest a key role of the anion nature in determining the type of behavior, and consequently, a complex dissolution mechanism should be expected. Nevertheless, this subject has not been properly explained yet.

More recently, Anik et al. [7] have investigated the anodic WO_3 dissolution by employing a rotating disk electrode. Their findings indicate that tungsten oxide dissolution exhibits a mixed control (at the oxide surface and by diffusion of soluble species) in the $0 < pH < 7$ range.

Dissolution of oxide films is mainly governed by a decrease in thickness, although the influence of hydration stages and/or generation of porosity/roughness can also affect the whole process. We have shown that in situ ellipsometry allows characterizing the conditions under which oxide dissolution is mainly governed by layer thinning.[1] The present work reports our ellipsometric study of the chemical dissolution of anodic WO_3 films in aqueous solutions performed with the objective of outlining the relevant features of its reaction mechanism. A thorough discussion of our results is presented in five sections. In section 3.1, the methodology developed to obtain kinetic information from the ellipsometric data is described, discussing the general criterion to determine the applicability of the anisotropic single-layer model (ASLM). In section 3.2, the rate law dependence on oxide thickness is analyzed by contrasting capabilities of capacitance measurements and ellipsometry and by discussing the physicochemical interpretation provided by the different rate laws. In section 3.3, the experimental evidence that indicates the existence of a hydration step during anodic WO_3 dissolution is discussed in detail. The discussion in section 3.4 is focused on drawing the main features of the mechanism of anodic WO_3 dissolution. The final section, 3.5, deals with the role that anion nature may play in the dissolution of anodic WO_3.

2. Experimental Section

The working electrode consisted of a polycrystalline tungsten rod (Koch-Light, 99.999% purity), 4 mm in diameter, mounted in a Teflon holder, with a geometric area of 0.126 cm^2. All potentials were measured relative to a $Hg|Hg_2SO_4|$ 1 M Na_2SO_4 reference electrode, but in the text they are referred to the standard hydrogen electrode (SHE). A platinum sheet with 9 cm^2 of geometric area was used as the counter electrode. Measurements were performed at 25 °C, in aqueous solutions of constant ionic strength, prepared from AR chemicals, and purified water with a resistivity of 18 MΩ cm (Milli Ro-Milli Q system). Different acids (HCl, H_2SO_4, H_3PO_4, and acetic (HAc)) were used to study the dissolution of anodic WO_3 films grown in solutions of different composition. Electrolytic solutions consisted of a mixture of the acid (HA) and its sodium salt (NaA) at 1 M total concentration (x M HA + $(1 - x)$ M NaA, with $0 < x < 1$). Electrochemical measurements were carried out using a 173 EG&G PARC potentiostat-galvanostat coupled to a 175 EG&G PARC signal generator and a 7090A Hewlett-Packard plotting recorder. All solutions used were deaerated by bubbling nitrogen before the oxide growth. Bubbling was stopped to avoid uncontrolled convection during film growth and dissolution, keeping the cell in a nitrogen atmosphere.[8,9]

* To whom correspondence should be addressed. E-mail: mperez@fisquim.fcq.unc.edu.ar; Fax: +54 351 4334188.

10.1021/jp051102k CCC: $30.25
Published on Web 09/27/2005

Optical measurements were performed with a Rudolph Research rotating-analyzer automatic ellipsometer (vertical type, 2000 FT model), equipped with a 75 W tungsten lamp as the light source and a filter (546.1 nm). The in situ ellipsometric experiments were done in a three-compartment cell (Pyrex glass) of 150 mL. The working electrode was mounted on a Teflon holder and placed horizontally in the central cell compartment, which has two plane glass windows adequate for optical measurements. The incidence angle used for all experiments was 70.00°.[1]

The working electrode was pretreated in a three-step procedure starting with mechanical polishing, performed to obtain a flat reflective surface, which consisted of emery paper abrasion followed by mechanical polishing with 9 μm diamond paste on a Texmet (Buehler) polishing pad. Next, an anodic WO_3 film was galvanostatically grown at a current density of 2 mA cm^{-2} in a solution of 5×10^{-3} M H_2SO_4 + 0.995 M Na_2SO_4 (growth step). The growth process was followed by in situ ellipsometry and by measurement of the potential transient. The electroformed oxide film was chemically dissolved by immersion in 0.1 M NaOH solution for 3 s (chemical etching step). Growth and dissolution were repeated 9−12 times until a reproducible ellipsometric curve for the oxide growth was obtained. The growth of WO_3 films on mechanically polished surfaces exhibits electrochemical and ellipsometric behavior different from that observed on chemically pretreated surfaces. Usually, the first type of surfaces presents film breakdown at low potential values (6−10 V) which is not observed until reaching 50−60 V on chemically pretreated surfaces. The changes in the shape of the ellipsometric curve obtained in each oxide growth step are also a clear indication of small, though noticeable, differences in the oxide optical properties. The mechanical abrasion produces tensions in the electrode surface that strongly influence the electrochemical and optical properties of the grown oxide films on it. Therefore, ellipsometric reproducibility between two successive growth steps is an indication that the oxide properties are constant and that the pretreatment has allowed the removal of tensions in the surface electrode.

The anodic growth of WO_3 films was performed galvanostatically up to 50 V (ca. 125 nm in thickness) in all cases by applying a current density of 2 mA cm^{-2}, in several formation media varying the electrolyte (H_2SO_4/Na_2SO_4, H_3PO_4/NaH_2PO_4, HCl/NaCl, and HAc/NaAc) and the composition. The chemical dissolution of the anodic WO_3 films was monitored ellipsometrically at the open circuit potential in the formation electrolyte.[8,9] To analyze the differences in the optical behavior as the anodizing field is removed, the circuit was opened for some seconds at regular time intervals during the oxide growth. To minimize the dissolution effect on the film thickness, the time elapsed between circuit openings and current reconnections was fixed at 20 s. This procedure makes it possible to determine the optical constants and thickness values of the oxide film at the anodizing field value or at zero field and, also, to analyze the change in properties as the field is switched on and off. This procedure was systematically applied to perform the optical measurements in each formation medium studied. As it will be shown in the next section, such a procedure enables the determination of a useful experimental reference for each particular electrolyte composition that helps to analyze the dissolution optical response.

The optical data were fitted by employing an anisotropic single-layer model (ASLM) that assumes the anodic WO_3 film to be a single layer of constant optical properties that grows on a flat bare tungsten substrate. The fitting model uses the Simplex method[9] to minimize the function 1

$$G = \frac{1}{m}\{\sum_{i=1}^{m}[(\Delta_i - \Delta_i^c)^2 + (\Psi_i - \Psi_i^c)^2]^{1/2}\} \qquad (1)$$

where the superscript "c" of Δ and Ψ denotes the values calculated by the model. No assumptions on the values of the optical properties were made in fitting the experimental response, allowing the Simplex algorithm to vary six parameters, namely, the refractive index (n) and the extinction coefficient (k) for the oxide-free flat substrate (n_s, k_s) and the corresponding film properties in the parallel (n_{xy}, k_{xy}) and the normal (n_z, k_z) directions to the surface substrate. Film thickness is an additional parameter that is optimized in the fitting process, though its variation is constrained by the set of values of (n_{xy}, k_{xy}, n_z, k_z, n_s, k_s) that is being assessed in each iteration step. For the cases in which the optical response can be described in terms of this model, the fitting procedure allows the optical properties and thickness of the oxide films to be obtained. The root-mean-square (rms) deviations were typically of 0.02°.

3. Results and Discussion

3.1. Optical Analysis. The growth of anodic oxides on "valve metals", like tungsten, takes place via an ionic conduction mechanism caused by a "high field",[11] and the potential drop occurs mainly across the oxide film. For anodic tungsten oxide (WO_3), an important effect of the magnitude of the anodizing electric field on the oxide properties was reported for films grown in aqueous solutions[1,8,9] and in acetic acid with 2% of water saturated with sodium tetraborate.[12,13] We have previously demonstrated[1] that the determination of the ellipsometric response completely governed by a change in thickness under open circuit (OC) conditions is the key to distinguishing among different processes that take place during oxide dissolution. Consequently, the growth of anodic WO_3 films was ellipsometrically characterized under both anodizing and OC conditions by performing the growth procedure described in the Experimental Section.

Ellipsometric $\Psi-\Delta$ response for the growth of an anodic WO_3 film in a 0.7 M HAc + 0.3 M NaAc solution up to a final thickness of ca. 125 nm is shown in Figure 1. The starting point corresponds to the optical response of the tungsten substrate covered with a very thin oxide layer (thickness $\approx$ 0 nm). The $\Psi-\Delta$ values obtained after the circuit openings at different thickness values during oxide growth are also shown. These OC data correspond to the optical response that defines the optical properties of the anodic WO_3 film in the absence of the electric field.[1] The arrows indicate the direction in which the optical response evolves with time for increasing thickness under both conditions. For the sake of clarity, several thickness values are indicated. The differences between the data corresponding to OC and to anodizing conditions are associated with the change of the optical properties caused by the presence or absence of the electric field.[1,8,9] Both sets of data can be interpreted in terms of the ASLM, yielding low fitting error and reliable values for the optical properties and thickness. This indicates that the optical response under each condition is fully determined by the increase in thickness, while the optical properties of the film are constant during growth. Refractive index values, obtained under anodizing conditions ($n_{xy} = 2.080$, $n_z = 2.196$) and under OC conditions ($n_{xy} = 2.100$, $n_z = 2.280$), indicate that anodic WO_3 films are anisotropic in nature irrespective of the electric field.[8] The values obtained for the

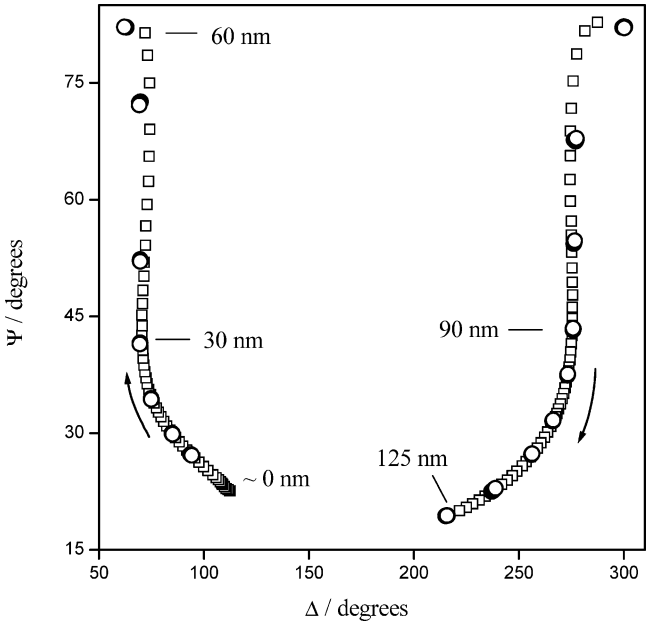

Figure 1. Ψ−Δ response during the anodic growth of WO_3, (□) under anodizing and (○) under OC conditions: $j = 2$ mA cm^{-2}; 0.7 M HAc + 0.3 M NaAc, pH = 3.9.

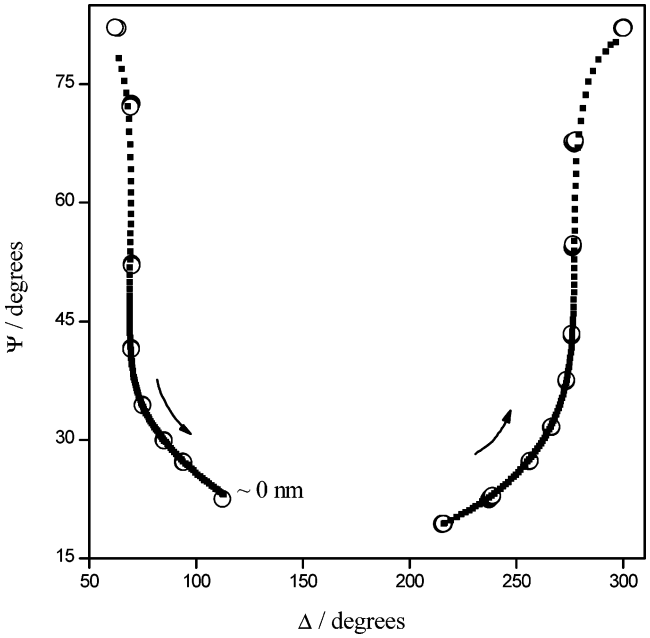

Figure 2. (■) OC Ψ−Δ response during the dissolution of a 125 nm thick anodic WO_3 film in a 0.7 M HAc + 0.3 M NaAc and pH = 3.9 solution. (○) OC Ψ−Δ response during the oxide growth under galvanostatic control ($j = 2$ mA cm^{-2}).

extinction coefficients (k_{xy}, k_z) are very small ($k \approx 0$) in both cases, showing that the films are transparent. Analyses of the values obtained for the optical properties of the anodic WO_3 in the different formation media indicate that they are practically constant and independent of the pH and electrolyte composition.

Although the decrease in thickness is the main process during oxide dissolution, processes such as hydration and generation of porosity/roughness of films may also occur. Accordingly, the contribution of each process to the response during dissolution must be evaluated to determine their relative importance. For ellipsometry, we have shown that the OC Ψ−Δ response can be used as a reference to ascertain the influence of other processes taking place simultaneously with oxide thinning.[1] The OC Ψ−Δ data obtained for increasing thickness during the WO_3 growth (Figure 1) can be interpreted as a thickness decrease when considered in the opposite direction. Therefore, if only oxide thinning takes place during dissolution, then the optical response must retrace the reference OC data profile. Hereafter, this data set will be referred to as "reference open circuit data" (ROCD).

To illustrate this assertion, Figure 2 shows the OC Ψ−Δ response obtained during the dissolution of an anodic WO_3 film, 125 nm thick, in a 0.7 M HAc + 0.3 M NaAc solution as compared to the ROCD. The arrows indicate evolution of the optical response with time during oxide dissolution. The response during dissolution goes backward, retracing completely the ROCD. This remarkable reversibility indicates, on one hand, that the optical response during dissolution is mainly determined by a thickness decrease and that the influence of other processes is very small or negligible. On the other hand, it also indicates that the dissolution response and the ROCD are characterized by the same values of optical properties. Accordingly, the dissolution response can be analyzed in terms of the ASLM and the thickness−time dependence can be obtained in the entire thickness range ($0 < d < 125$ nm).

Figure 3 shows the thickness−time dependence for dissolution of anodic WO_3 films in HAc/NaAc solutions of two different compositions in the whole 0−125 nm range. The linear dependence clearly indicates that dissolution rate is constant

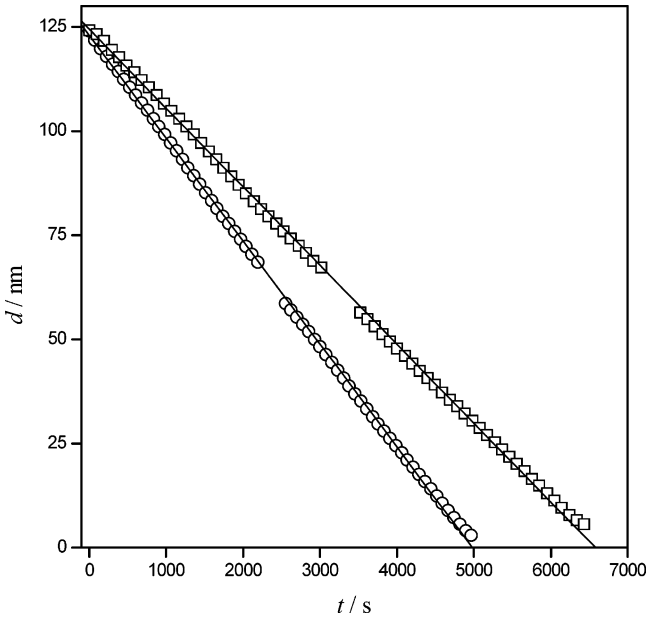

Figure 3. Thickness−time dependence during dissolution of anodic WO_3 in HAc/NaAc solutions of different composition. [HAc]: (○) 0.7 M (pH = 3.9) and (□) 0.8 M (pH = 3.7).

within the entire range and that dissolution kinetics obeys a zero-order law with respect to thickness. The same rate law was obtained in H_2SO_4/Na_2SO_4, H_3PO_4/NaH_2PO_4, and HCl/NaCl solutions of constant ionic strength in the $0 < pH < 6$ range, indicating that the order of the rate law with respect to thickness is independent of the specific nature of anions in the electrolyte.[1] From linear fitting of the thickness−time dependencies, dissolution rate values of 0.0189 and 0.0247 nm s^{-1} were obtained for [HAc] = 0.8 and 0.7 M, respectively.

The relative importance of other processes taking place simultaneously with the thickness decrease depends on the dissolving medium. Accordingly, the change in the electrolyte composition leads to Ψ−Δ responses with a shape different

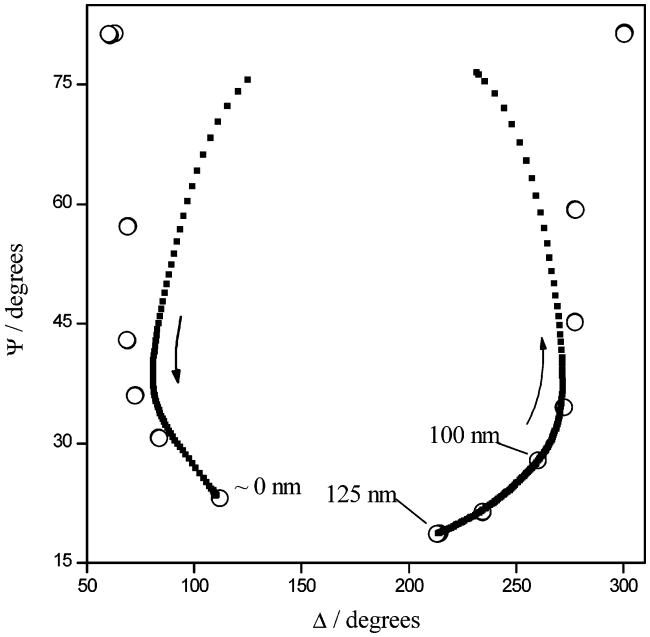

Figure 4. (■) OC Ψ−Δ response during the dissolution of anodic WO_3 in a 0.9 M HAc + 0.1 M NaAc and pH = 3.3 solution and (○) Ψ−Δ ROCD.

from that of the one shown in Figure 2. Figure 4 shows the OC Ψ−Δ response during the dissolution of an anodic WO_3 film, 125 nm thick, in a 0.9 M HAc solution as compared with the corresponding ROCD. For 0−1900 s, the dissolution response evolves backward retracing the ROCD. At times longer than 1900 s, the optical response gradually deviates, defining a path aside from the ROCD. This indicates that the Ψ−Δ response is a result of the interplay between thickness decrease and additional processes which will be analyzed in the sections below. Under these conditions, the Ψ−Δ response cannot be interpreted in terms of the ASLM over the entire thickness range. Additional phenomena produce changes in the optical properties of the film, which would yield multilayer structures. In principle, the entire optical response should be interpreted via multilayer models that consider changes in both optical properties and thickness for each layer. Nevertheless, it is still possible to obtain quantitative thickness−time information in a restricted range of either thickness or time. Since the conclusions derived from the reversibility do not depend on the thickness range where it is observed, the dissolution response in the 0−1900 s range is mainly determined by thickness decrease and it is also characterized by the same optical properties as ROCD. The optical reversibility within the 0−1900 s range allows the ASLM to be applied to obtain the thickness−time dependence in the 100−125 nm range. To help convergence in fitting, ad-hoc data sets were built up by linking the dissolution Ψ−Δ response showing reversibility and the ROCD. The fitting error values obtained for this kind of data sets were similar to those obtained for the ROCD, a fact that pleads in favor of the build-up procedure. This also indicates that, in this restricted thickness range, the optical response is mainly determined by the thickness decrease and is not very much affected by the additional processes.

In summary, the criterion based on the optical reversibility of the dissolution response[1] was broadened to be applied in general, whether the reversibility is observed in the entire or a restricted thickness range. Therefore, reliable thickness−time dependencies can be obtained by applying the ASLM either in the whole range of thickness or in a narrower thickness range depending on the composition of the formation electrolyte.

3.2. Dissolution Rate Law. In this section, we will analyze the reasons for the discrepancy found on the thickness order in the rate law, between our results and those previously reported.[3,6] To do so, we will address this subject by analyzing the suitability of capacitance measurements for studying the oxide dissolution and by criticizing the physicochemical interpretations derived from the different laws.

Two aspects are important to analyze capacitance measurement: the experimental conditions and the interpretation of the results. First, capacitance is obtained under polarization conditions, frequently at OC potential, and this might be one cause of the different kinetic dependencies observed. Regarding the second aspect, the capacity response during dissolution is interpreted as changes in the film thickness occur, assuming that the interphase behaves as a single condenser of parallel plates. Nevertheless, this type of measurements would provide reliable information on thickness only when oxide dissolution proceeds exclusively as film thinning. When hydration and/or roughening occur, the capacitance should include the contribution of such processes. Thus, capacitance measurements performed in HAc/NaAc and H_2SO_4/Na_2SO_4 solutions yielded a first-order law instead of a zero-order law as the ellipsometric measurements showed. In contrast with capacitance measurements, ellipsometry is a suitable method to follow oxide dissolution under OC conditions (without polarization) and also allows for distinguishing among the different processes involved in the overall oxide dissolution, giving reliability to the thickness−time dependencies determined.[1]

Regarding the physicochemical interpretation of rate laws, it is important to notice that, for a heterogeneous reaction like oxide dissolution, the rate law should be written in terms of the activities of the reacting species at the oxide/solution interface. The dependence of the rate law on the activity of the species promoting dissolution could be accounted for either by the bulk or by the surface concentration, depending on which process is the rate-determining step. The oxide itself, as the other reactive species, should have an activity at the oxide/electrolyte interface independent of any diffusion or adsorption process. This activity should depend on the surface density of active sites for the adsorption of dissolving species and on the real area exposed at that interface. If the area is constant, then the oxide activity may be constant during the oxide dissolution and, therefore, the rate law should not depend on oxide activity. Thus, a rate law involving first-order dependence on thickness is inconsistent from a physicochemical viewpoint. If film thickness describes oxide activity, then such a parameter will take into account the activity not only at the interface but also in the bulk. Consequently, that dependence on thickness would indicate that a heterogeneous reaction taking place at the oxide/electrolyte interface is controlled by the bulk oxide activity beyond the interface. Such an interpretation would be clearly inconsistent.

If the dependence of rate law on thickness could be associated with the experimental conditions used in capacitance measurements, where the potential applied could be thought as the link between oxide activities in the bulk and at the interface, then some major points should be addressed. First, reasonable arguments on the suitability of thickness for describing the bulk oxide activity should be provided. Second, if this point has been overcome, then the dependence on thickness should be interpreted as the result of a rate controlled by diffusion or migration through an oxide film, in equivalence with how a rate law written in terms of bulk concentration of soluble species would be read. Since the electric field across the film is expected to be very small, neither diffusion nor migration should fit the

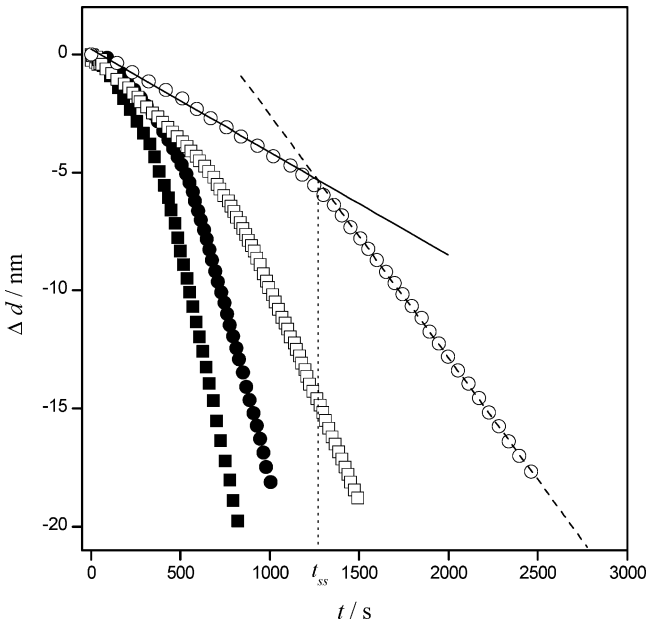

Figure 5. Decrease of thickness−time dependence for H_3PO_4/NaH_2PO_4 solutions with different composition. $[H_3PO_4]$: (○) 1×10^{-1} M (pH = 2.5), (□) 1×10^{-2} M (pH = 3.6), (●) 2×10^{-3} M (pH = 4.6), and (■) 2×10^{-4} M (pH = 5.3), with $[H_3PO_4] + [NaH_2PO_4] = 1$ M.

time scale in which dissolution takes place. Finally, even when the aspect pointed out could be properly addressed, it will be necessary to accept that the dependence observed depends on the technique used (i.e., capacitance measurement).

Another possible cause of the rate law dependence on thickness could be associated with different chemical properties or structure (bilayers) of films prepared under different conditions or by different methodologies. It is expected that anodic oxide films would exhibit different behavior from those obtained by precipitation or CVD. In the particular case of anodic WO_3 films prepared under galvanostatic control, different values of current density would lead to films with a different degree of aging or density. If that were the origin of a rate law which depends on thickness, then the same rate law should be obtained irrespective of the monitoring techniques used. Since the discrepancies remain for anodic WO_3 films obtained under similar conditions (under galvanostatic control at 1.6 mA cm^{-2} in ref 3 and at 2 mA cm^{-2} in the present study), the preparation of films as the cause of the discrepancies must be rejected.

Therefore, the rate law independent of the oxide thickness should be, from the physicochemical viewpoint, the only one suitable for describing the dissolution of anodic oxide films under OC conditions (i.e., zero field). Hydration and generation of porosity/roughness can affect the oxide activity at the interface, although their effect on kinetic behavior will be analyzed in detail below.

3.3. Early Stages of Dissolution of Anodic WO_3. Kinetic information corresponding to the studied electrolytes was obtained, according to the procedure described in section 3.1. Thickness−time dependencies (d/t) provide kinetic information over the entire or a restricted thickness range depending on the total or partial reversibility found in each case. As a rule, dissolution of anodic WO_3 appears to obey a rate law independent of film thickness for all electrolytes. However, a singular behavior is detected at the beginning of oxide dissolution. For the sake of clarity, results will be analyzed in terms of the decrease in thickness, Δd, defined as $\Delta d(t) = d(t) - d_f$, where d_f is the final thickness after oxide growth. Figure 5 shows the $\Delta d/t$ dependence obtained during dissolution of anodic WO_3 in H_3PO_4/NaH_2PO_4 solutions of different concentrations. The $\Delta d/t$ dependence was obtained from fitting either in the whole range of thickness (i.e., from −125 to 0 nm, for $[H_3PO_4] = 1 \times 10^{-2}$ to 2×10^{-4} M) or within a narrower thickness range depending on the composition. Nevertheless, $\Delta d/t$ data are displayed in the −20−0 nm range to show on a magnified scale the singular behavior observed at the beginning of the dissolution. Two approximately linear regions can be observed for each composition. The first region extends from the circuit opening ($t = 0$) up to a time value (t_{ss}) at which the slope changes noticeably, producing a break in the $\Delta d/t$ dependence, while the second region corresponds to time values greater than t_{ss} (indicated in the figure for $[H_3PO_4] = 1 \times 10^{-1}$ M). The t_{ss} value increases with H_3PO_4 concentration, while the corresponding Δd value remains constant at around −5 nm. The change in slope indicates the rate modification of the oxide dissolution, determined by the change in the relative influence of the different processes involved. At the beginning of oxide dissolution, additional processes may occur simultaneously with thickness decrease. Nevertheless, since every d/t dependence was determined from the reversible dissolution response which is mainly governed by thickness decrease, the effect of the additional processes can be assumed very small. If this assumption was not correct, then the dissolution response would exhibit a deviation from the ROCD. Moreover, since the additional processes appear to be independent of the nature of electrolyte anion or pH since the same type of behavior is obtained in H_2SO_4/Na_2SO_4, HAc/NaAc, and HCl/NaCl solutions of different composition, we will associate them with a hydration step.

Some authors have proposed the hydration of electroformed WO_3 films as a step among the processes involved in the oxide dissolution mechanism,[2,14] while others believe that the electroformed oxide is hydrated in nature, $WO_3 \cdot H_2O$, either in a thin layer at the oxide/electrolyte interface or in the whole thickness film.[15−17] To analyze the beginning of the dissolution of anodic WO_3, we will assume that the electroformed oxide is initially anhydrous. This assumption is in opposition with previous findings,[2,14−17] given that our experimental conditions are quite different. In the majority of these works,[14−17] anodic WO_3 was studied under steady-state conditions, exposing oxide films to the hydration during long times. With regards to that, the question remained whether the hydrated films were obtained during the formation or in the long periods of time elapsed during the experiments. In the present study, on the contrary, the dissolution optical response corresponds to films exposed to hydration only during the time needed for them to grow (from 6 to 8 min). In accordance with such an assumption, the first region would correspond to the generation of an external thin hydrated layer at the oxide/electrolyte interface, according to eq 2

$$WO_{3(s)} + H_2O_{(l)} \rightarrow [WO_3 \cdot H_2O]_{(s)} \qquad (2)$$

yielding a bilayer structure composed of an inner WO_3 layer and an outer $WO_3 \cdot H_2O$ one. During this stage, the outer hydrated layer grows in thickness at the expense of the underneath anhydrous layer, while the total thickness of the bilayer decreases as a consequence of the dissolution (Figure 6a). Although the hydration leads to a bilayer structure, the optical reversibility indicates that the thickness reached by the external layer is very small compared to the total bilayer thickness. This assumption is corroborated by the small error values obtained from the optical data fitting with the ASLM, which are an indication that the bilayer structure must be close to that of a

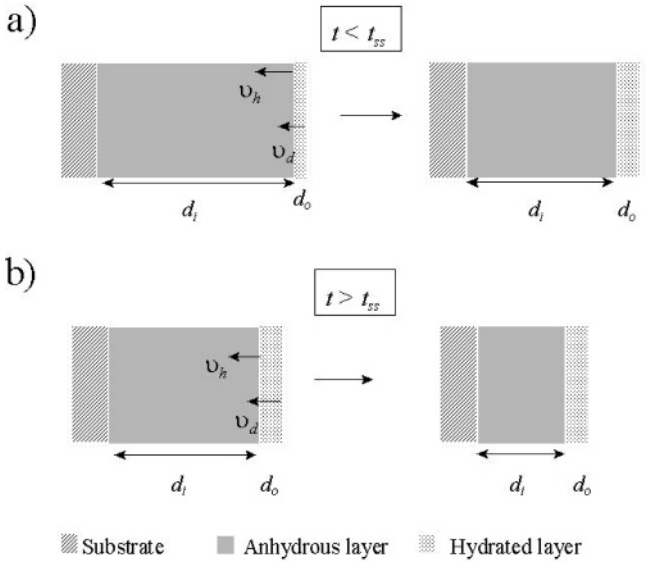

Figure 6. Scheme of the contributions of hydration and thickness decrease of the total bilayer with increasing time: (a) in the $0 < t < t_{ss}$ range, the outer hydrated layer grows up at the expense of the inner anhydrous layer while the bilayer thickness decreases, and (b) for $t > t_{ss}$, the thickness of the inner anhydrous layer decreases whereas the thickness of outer hydrated layer is in a stationary state ($\upsilon_h = \upsilon_d$). υ_h and υ_d are the rates corresponding to the hydration and dissolution processes, respectively, while d_i and d_o correspond to the thickness values of the inner anhydrous oxide layer and the outer hydrated oxide layer, respectively.

single layer. The generation and growth of the hydrated layer would slightly influence the optical response at the beginning of the dissolution, that is, in the $0-t_{ss}$ time range. For time values greater than t_{ss}, the contribution of the hydration process and thickness decrease of the bilayer cancel each other, providing a stationary thickness of the hydrated layer (Figure 6b).

The change rate of the outer hydrated layer thickness (d_o) and the inner anhydrous layer thickness (d_i) can be expressed in terms of the rates of the hydration process (υ_h) and the change of thickness of the bilayer (υ_d), as (eqs 3 and 4)

$$\left(\frac{\partial d_o}{\partial t}\right)_t = -\upsilon_d(t) + \upsilon_h(t) \tag{3}$$

$$\left(\frac{\partial d_i}{\partial t}\right)_t = -\upsilon_h(t) \tag{4}$$

where the absolute rate values (υ_h and υ_d) were considered. The contribution of each process is represented in Figure 6a. The rate of hydration (υ_h) should be controlled by the oxide and water activities at the oxide/solution interface, which do not depend on dissolution time. It is therefore expected that the hydration process has a constant rate. On the other hand, the change in thickness of the bilayer (υ_d) should depend on the activity of the dissolving species at the outer hydrated layer/solution interface, which could be controlled by either adsorption or diffusion processes. Therefore, υ_d should exhibit a time dependence during the dissolution. For $t < t_{ss}$ and $\upsilon_d < \upsilon_h$, according to eq 3, the thickness of the outer layer increases with time ($\partial d_o/\partial t > 0$). For $t > t_{ss}$, d_o reaches a steady-state value (eq 5)

$$\left(\frac{\partial d_o}{\partial t}\right)_{t>t_{ss}} = 0 \tag{5}$$

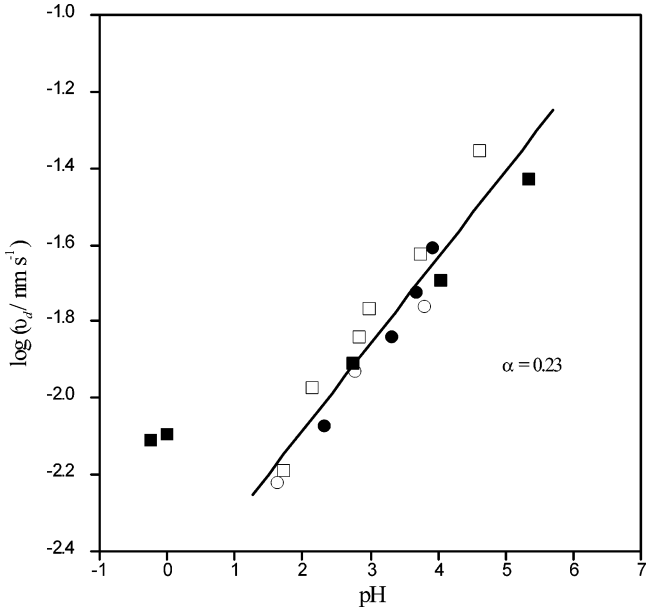

Figure 7. log(υ_d) vs pH dependence for different electrolyte solutions: (■) $[H_3PO_4] = 1.7$ M (∗), 1 M, 1×10^{-1} M, 1×10^{-2} M, 2×10^{-3} M, with $[H_3PO_4] + [NaH_2PO_4] = 1$ M except for (∗); (□) $[H_2SO_4] = 1 \times 10^{-1}$ M, 5×10^{-2} M, 1×10^{-2} M, 5×10^{-3} M, 1×10^{-3} M, 1×10^{-4} M, with $[H_2SO_4] + [Na_2SO_4] = 1$ M; (●) [HAc] = 1.0 M, 0.9 M, 0.8 M, 0.7 M, with [HAc] + [NaAc] = 1 M; (○) [HCl] = 1×10^{-2} M, 1×10^{-3} M, 1×10^{-4} M, with [HCl] + [NaCl] = 1 M.

From eq 3, for $t > t_{ss}$ (eq 6)

$$\upsilon_d(t > t_{ss}) = \upsilon_h(t > t_{ss}) \tag{6}$$

For $t > t_{ss}$, from eqs 4 and 6

$$\left(\frac{\partial d_i}{\partial t}\right)_{t>t_{ss}} = -\upsilon_d(t > t_{ss}) \tag{7}$$

According to eq 7, once d_o has reached a stationary value, the thickness decrease rate of the inner anhydrous layer is the same as the rate of the bilayer thickness decrease. This is in agreement with the facts that d_o should correspond to a very small fraction of the bilayer and that the thickness decrease of the inner anhydrous layer (the thickest layer) should be the one that governs the $\Psi-\Delta$ response. Under conditions in which the thickness of the outer hydrated layer has a stationary value, the hydration process influence does not have an appreciable effect on the $\Psi-\Delta$ response, which is governed in turn by the decrease of thickness of the inner anhydrous layer.

From the foregoing analysis, it follows that hydration has a slight but measurable influence on the optical response in the $0-t_{ss}$ time range only, whereas its influence does not have an appreciable effect on the $\Psi-\Delta$ response for times longer than t_{ss}. The time range $0-t_{ss}$ is what we call the early stages of oxide dissolution, and it corresponds only to a fraction of the whole time range where optical reversibility is observed, that is, where the $\Psi-\Delta$ response is mainly governed by the thickness decrease. The early stages of oxide dissolution, that take place in the first region of the $\Delta d/t$ plots in Figure 5 (ca. $\Delta d = -5$ nm), would correspond to the time necessary (t_{ss}) to attain the stationary thickness value of the outer hydrated layer, which is dependent on the pH of the electrolyte. Therefore, the slope of the $\Delta d/t$ plots in Figure 5 for $t > t_{ss}$ must be interpreted as the true oxide dissolution rate in the given media.

3.4. Dissolution Kinetics of Anodic WO_3 Films. The following schemes have been proposed for the dissolution

reaction of anodic WO_3 in alkaline and in acidic media, respectively[3−6]

$$WO_{3(s)} + 2\,HO^-_{(aq)} \rightarrow WO_4^{2-}{}_{(aq)} + H_2O_{(l)} \quad (8)$$

$$WO_{3(s)} + 2\,H^+_{(aq)} \rightarrow WO_2^{2+}{}_{(aq)} + H_2O_{(l)} \quad (9)$$

These overall reactions account for the dissolution as mainly determined by pH and independent of the specific nature of the electrolyte anion. Figure 7 shows the $\log(\upsilon_d)$−pH dependence for the dissolution of anodic WO_3 films in the investigated electrolytes, where υ_d is the dissolution rate determined ellipsometrically, according to sections 3.1 and 3.3. For pH > 1.5, in general, the dissolution rate increases with pH, indicating that dissolution is promoted by OH^-. Furthermore, dissolution rate is almost independent of the specific nature of the electrolyte anion. For concentrated H_3PO_4 solutions (pH ≈ 0), a departure from the general tendency is observed, indicating a likely change in the dissolution mechanism, probably involving H^+ as the dissolving species (eq 9). The OH^- reaction order of 0.23, obtained from the $\log(\upsilon_d)$−pH plot (Figure 7) for pH > 1.5, indicates that OH^- diffusion is not the rate-determining step. In accordance to this and to the hydration step proposed in section 3.3, the overall dissolution reaction 8 can then be expressed as

$$WO_{3(s)} + H_2O_{(l)} = [WO_3{\cdot}H_2O]_{(s)} \quad (2)$$

$$[WO_3{\cdot}H_2O]_{(s)} + OH^-_{(aq)} = [WO_3{\cdot}H_2O]_{(s)}\,(OH^-)_{(ad)} \quad (10)$$

$$[WO_3{\cdot}H_2O]_{(s)}\,(OH^-)_{(ad)} \rightarrow HWO_4^-{}_{(aq)} + H_2O_{(l)} \quad (11)$$

$$HWO_4^-{}_{(aq)} + OH^-_{(aq)} = WO_4^{2-}{}_{(aq)} + H_2O_{(l)} \quad (12)$$

Reactions 2, 10, and 11 take place at the oxide/electrolyte or the outer hydrated layer/electrolyte interface. Equation 10 accounts for the OH^- adsorption/desorption process, eq 11 corresponds to the decrease in the bilayer thickness, and eq 12 describes the subsequent acid−base equilibrium. Given the negligible influence of hydration for $t > t_{ss}$, the rate-determining step would correspond to the surface process accounted for by eq 11. Similar mechanisms have been previously reported for chemical dissolution of oxides of different metals (Be, Al, Ni, etc.).[18−21] When a process at an oxide surface corresponds to the rate-determining step, fractional or integer reaction orders are obtained when the dissolution rate law is expressed in terms of the dissolving species concentration in the bulk or at the surface, respectively. Accordingly, the fractional order reported here would indicate that the OH^- surface concentration controls dissolution rate. Such a result is in accordance with the control at the oxide interface that Anik et al. have found.[7] Although these authors report that dissolution is also controlled by diffusion of soluble species, this discrepancy with the conclusion obtained here could be associated with the differences in experimental conditions used in both studies.

Although the ultimate test of the rate law will be to determine the species concentration at the surface, the proposed reaction scheme summarizes all the outstanding features found for the dissolution of anodic WO_3 in different electrolytes, giving a new insight into the characterization of this reaction. Whereas the phenomenology previously reported in the literature[3−6] suggested a complex chemistry for dissolution of anodic WO_3, the present work would indicate that this reaction has many aspects in common with general dissolution mechanisms of oxides.

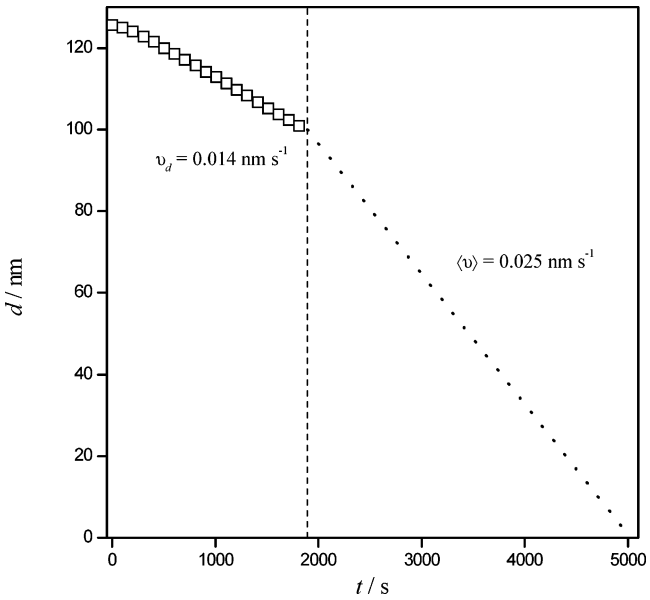

Figure 8. (□) Thickness−time dependence determined from fitting of the experimental data in the range 0 s < t < 1900 s, and (····) the average dependence calculated for the range 1900 s < t < 5100 s during dissolution of anodic WO_3 in 0.9 M HAc + 0.1 M NaAc, pH = 3.3.

3.5. Role of Anions Nature. The ellipsometric analysis hitherto presented indicates that the dissolution rate law is not determined by hydration, which has a slight influence during the early stages only. Except for OH^-, the rate law is practically independent of the specific nature of the electrolyte anion. However, this conclusion is valid only when the generation of porosity/roughness is negligible compared to thickness decrease. As the pH of the formation medium decreases, cases such as the one shown in Figure 4 are obtained where the development of porosity/roughness produces the strong deviation of the Ψ−Δ dissolution data from the ROCD (1900 s < t < 5000 s). Under these conditions, the interplay between thickness decrease and generation of roughness determines the shape of the optical response. Figure 8 shows the d/t dependence for the oxide dissolution under these particular conditions. On the left side of the vertical dashed line lies the only region where the ASLM can be applied to obtain $\upsilon_d = 0.014$ nm s^{-1}. Since the ASLM cannot be used within the 1900 s < t < 5100 s range, a dissolution average rate of $\langle\upsilon\rangle = 0.025$ nm s^{-1} (represented by the dotted line) was calculated from the oxide thickness remaining at 1900 s (100 nm) and from the assumption that the thickness is almost zero at 5100 s. The fact that $\langle\upsilon\rangle$ is almost twice the value of υ_d indicates that the generation of porosity/roughness at the oxide/electrolyte interface for t > 1900 s increases the area of the outer hydrated layer. However, this change in the dissolution rate is only apparent. A similar behavior has been observed in H_2SO_4/Na_2SO_4, H_3PO_4/NaH_2PO_4, and HCl/NaCl solutions as acid concentration is increased. In addition, $H_2PO_4^-$ appears to be the least aggressive anion. Under conditions in which the interplay between thickness decrease and the generation of roughness determines the response obtained by a given technique, the lack of an evaluation of the real area might result in a rate law that shows a dependence on thickness.[3,6]

In summary, electrolyte anions may participate only in favoring the generation of porosity/roughness as pH decreases. Under these conditions, the determination of accurate dissolution

rates can be achieved only if the dependencies of both thickness and area on time are known.

4. Conclusions

Ellipsometry has been successfully used as an in situ characterization technique to study the chemical dissolution of anodic WO_3 films in aqueous solutions.

The ellipsometry capabilities for distinguishing among thickness decrease, hydration, roughening, etc. have been successfully used to study the dissolution of anodic WO_3. The methodology employed helps to characterize the conditions of applicability of the ASLM. The optical analysis performed allowed us to determine the ranges of thickness within which reliable kinetic information can be obtained.

The rate law for dissolution of anodic WO_3 has been found to be independent of the oxide film thickness. This rate law provides a more correct physicochemical picture than the first-order rate law previously reported,[3,6] enabling us to conclude that the dissolution of oxide films in general should be formulated by means of a rate law independent of thickness.

A mechanism for the dissolution of anodic WO_3 has been formulated by including an initial hydration step which yields a bilayer structure at the interphase. For pH > 1.5, the dissolution rate is only determined by the surface concentration of OH^-, irrespective of the specific nature of the electrolyte anion. The fractional reaction order with respect to OH^- strongly suggests that the rate-determining step corresponds to a surface process. The role of the anions seems to be favoring the generation of porosity/roughness in anodic WO_3 films as pH decreases.

The present paper allowed us to put the dissolution of anodic WO_3 films on the same footing as general mechanisms used previously to describe dissolution of other metal oxides, such as Be, Al, and Ni oxides.[18−21]

Acknowledgment. This research has been financially supported by the Consejo Nacional de Investigaciones Científicas y Técnicas of Argentina, the Agencia Córdoba Ciencia S.E., and the Secretaría de Ciencia y Tecnología.

References and Notes

(1) Pérez, M. A.; López Teijelo, M. *Thin Solid Films* **2004**, *449*, 138.
(2) Arnoldussen, T. C. *J. Electrochem. Soc.* **1981**, *128*, 117.
(3) El-Basiouny, M. S.; Hassan, S. A.; Hefny, M. M. *Corros. Sci.* **1980**, *20*, 909.
(4) Hefny, M. M.; Mogoda, A. S.; El-Basiouny, M. S. *Corrosion* **1983**, *39*, 266.
(5) Hefny, M. M.; Gadalla, A. G.; Mogoda, A. S. *B. Electrochem.* **1987**, *3*, 11.
(6) Mogoda, A. S.; Hefny, M. M.; El Mahdy, G. A. *Corros. Sci.* **1990**, *46*, 210.
(7) Anik, M.; Osseo-Asare, K. *J. Electrochem. Soc.* **2002**, *149*, B224.
(8) Pérez, M. A.; López Teijelo, M. In *Passivity and its Breakdown*; Natishan, P. M., Isaacs, H. S., Janik-Czachor, M., Macagno, V. A., Marcus, P., Seo, M., Eds.; The Electrochemical Society Proceedings Series: Paris, 1997; PV 97-26, p 404.
(9) Pérez, M. A.; López Teijelo, M. *Eur. Fed. Corros.* **2000**, *28*, 206.
(10) De Smet, D. J.; Ord, J. L. *J. Electrochem. Soc.* **1989**, *136*, 2841.
(11) Dignam, M. J. In *Comprehensive Treatise of Electrochemistry*; O′M. Bockris, J., Conway, B. E., Yeager, E., White, R. E., Eds.; Plenum Publishing Corp.: New York, 1981; Vol. 4, p 247.
(12) Ord, J. L.; De Smet, D. J. *J. Electrochem. Soc.* **1992**, *139*, 359.
(13) Ord, J. L.; De Smet, D. J. *J. Electrochem. Soc.* **1992**, *139*, 728.
(14) Johnson, J. W.; Wu, C. L. *J. Electrochem. Soc.* **1971**, *118*, 1909.
(15) Di Paola, A.; Di Quarto, F.; Sunseri, C. *Corros. Sci.* **1980**, *20*, 1079.
(16) Di Paola, A.; Di Quarto, F.; Sunseri, C. *J. Electrochem. Soc.* **1980**, *125*, 1344.
(17) Lillard, R. S.; Kanner, G. S.; Butt, D. P. *J. Electrochem. Soc.* **1998**, *145*, 2718.
(18) Stumm, W.; Sulzberger, B.; Sinniger, J. *Croat. Chem. Acta* **1990**, *3*, 277.
(19) Stumm, W. In *Chemistry of Solid-Water Interface*; Wiley-Interscience: New York, 1992; p 157.
(20) Wieland, E.; Wehrli, B.; Stumm, W. *Geochim. Cosmochim. Acta* **1988**, *52*, 1969.
(21) Avena, M. J.; De Pauli, C. P. *Colloids Surf.* **1996**, *108*, 181.